Transport through driven systems - Application to Floquet topological states

Pedro Ninhos[1], Miguel A. N. Araújo[1,2], and Pedro Ribeiro[11,2]

[11] *CeFEMA, Instituto Superior Técnico, Universidade de Lisboa, Av. Rovisco Pais, 1049-001 Lisboa, Portugal*
[22] *Departamento de Física, Universidade de Évora, P-7000-671, Évora, Portugal*

This thesis investigates the interplay between two topics: electrical transport and driving-induced (Floquet) topological systems. Specifically, we study the role of topology on the transport properties of one-dimensional Floquet systems. This naturally leads us to investigate the role of symmetries on charge and heat pumping.

We consider a driven Su-Schrieffer-Heeger (SSH) chain. The average current as a function of the oscillation amplitude was found to be monotonic in the non-topological phase whereas in the topological phase it is non-monotonic.

We also address bound-state-induced transport by monitoring the transmission peaks when the chemical potentials lie inside the energy gap in an inhomogeneous setup. The increase in the number of localized states enhances the conductance due to electronic tunneling through those states.

Finally, we investigate charge and heat pumping in two models belonging to the BDI symmetry class. The presence of particle-hole symmetry (PHS) implies that the pumped charge (heat) is an odd (even) function of the chemical potential. This occurs if spatial symmetry (PS) is broken. If PHS is broken, the product of PHS with PS produces even/odd charge/heat pumping. An additional symmetry that behaves like a PHS, although not the usual one, is introduced, which renders the pumped charge/heat an odd/even function. Our results provide a simple criterion for reversing (or maintaining) the direction of the charge or heat flux.

Keywords: Floquet Systems, Topological Insulator, Transport, Symmetries

I. INTRODUCTION

One goal of Condensed Matter Physics is to classify the states of matter according to the properties of the system. Usually we are taught that we can find matter in three phases: gas, solid and liquid. Eventually we are told about the plasma state. However, this picture is a little bit reductive. In fact, there are many more states of matter that can be identified, such as superfluids, superconductors, liquid crystals or the Bose-Einstein condensate, and topological phases of matter. While topological phases of matter in equilibrium are well established, the same can not be said about non-equilibrium ones, object of current and active research.

Periodic driving of a topologically trivial system can render it topological [1], providing an alternative route to synthesize and manipulate topological nontrivial materials.

Topological insulators have been realized in experiments [2], one example being HgTe/CdTe quantum-wells [3], providing evidence for the quantum spin Hall effect. Other works searched for the quantized anomalous Hall (QAH) effect in tetradymite semiconductors Bi_2Te_3, Bi_2Se_3, and Sb_2Te_3 doped with transition metal elements (Cr or Fe) [4], which are known to belong to the class of topological insulators. The observation of the QAH effect has already been reported [5]. However, the choice of materials that exhibit these unique topological properties remains rather scarce.

Fortunately, external periodic driving opens a route to engineer that kind of topological materials from materials that are topologically trivial in equilibrium. The materials that display topological properties under periodic driving are usually called Floquet topological insulators (FTIs) [6]. One example is a graphene ribbon attached to two electrodes (one in each edge) and irradiated by circularly polarized light as described in a work by T. Oka and H. Aoki [7]. Moreover, we can find in the literature reports of experimental realizations involving graphene, namely in Ref. [8], where the driving induces the Haldane model [9].

Transport along one dimensional driven systems has been studied by P. Hänggi *et al.* in Ref. [10], where a Floquet Green function approach was adopted. In Ref. [10] and in this work the thermalization mechanism is due to the contact with two leads.

Transport properties of Floquet topological phases in one dimension has been reported by O. Balabanov and H. Johanesson in [11]. Predictions for transmission spectra are presented. Namely, peaks in the transmission spectra that lie in the gaps whenever the system is in a topological phase are observed. The height of the peaks depends non-monotonically with the chain size. In this work we extend the analysis to non-homogeneous chains, with two portions of the chain being driven with different amplitudes.

In the context of quantum charge pumping, symmetries play a huge role. Both [12] and [13] point out that to obtain a pumped current the left-right symmetry of the system must be broken. This can be achieved by breaking parity (or spatial) symmetry (PS) or time-reversal symmetry (TRS).

In this work the main goal is to establish transport properties of Floquet topological phases in one dimension. For that we compute the average current and the differential conductance for different topological phases of two distinct models. We study the implications symmetries have on the charge pumping for two distinct mod-

els as well. The tools acquired also allow for the study of the heat pumping for the models already considered in the charge pumping.

This paper is organized as follows. In Sec. II we discuss the setup of our physical system and introduce the tight-binding models we will work on. In Sec. III we present the phase diagram of the Magnus effective Hamiltonian of the first model introduced in II, using the winding number for static systems, and the phase diagram of the second model introduced in II using the winding number for Floquet systems. In section IV we explain briefly how to compute the average charge current, the total heating of the leads and the pumped heat between them. We also define the transmission coefficients to be studied. In section V we start by computing the average current as a function of the driving amplitude for the first model introduced. Then we move on to the second model, where we compute the transmission peaks for homogeneous and inhomogeneous chains varying the chain size, and compare the results between the two cases. In the first situation we compute the transmission peaks at zero energy and in the second we study the transmission peaks at $\pm\pi$ energies. In section VI we study the role symmetries have on the even/odd behavior of the charge pumping, using the second and third models introduced in section II. In section VII we study the role symmetries have on the even/odd behavior of the total heating of the leads and the heat pumping between the leads, using again the second and third models introduced in section II. We finish with section VIII, where we make conclusions and final remarks.

II. SETUP AND MODELS

In this work we consider one dimensional tight-binding models driven by an external time-periodic field. This can be achieved by illuminating the chain with radiation, which in our case would be monochromatic. The electrodes are metallic leads connected to a battery which sets a bias V between them. The leads, which act as reservoirs, are connected to the chain through the end sites. The left lead is at the chemical potential μ_L and the right one at the chemical potential μ_R. The bias applied is thus $V = (\mu_R - \mu_L)/e$, $e > 0$.

In this work we consider three models. The first one is a driven version of the Su-Schrieffer–Heeger (SSH) model, with Floquet Bloch Hamiltonian

$$\begin{aligned} H(k,t) =&(t_1 + t_2\cos k)\ \sigma_x + (t_2 \sin k - 2A\sin(\Omega t))\ \sigma_y + \\ &2A\cos(\Omega t)\ \sigma_z\,, \end{aligned} \tag{1}$$

where A and Ω are the amplitude and frequency of the driving, respectively, t_1 and t_2 are the hopping amplitudes of the static SSH model, and σ_x, σ_y and σ_z are the three Pauli matrices, acting on the sublattice space. The second model is a variant of the driven SSH chain, which we called zx model:

$$H_{zx}(k,t) = (\sin k, 0, \cos k + A\cos(\Omega t) + \mu)\cdot(\sigma_x,\sigma_y,\sigma_z)\,. \tag{2}$$

The last and third model is obtained from (2) by a cyclic permutation of the Pauli matrices. We called it xy model:

$$H_{xy}(k,t) = (\cos k + A\cos(\Omega t) + \mu, \sin k, 0)\cdot(\sigma_x,\sigma_y,\sigma_z)\,. \tag{3}$$

III. TOPOLOGICAL PHASE DIAGRAMS

A. Symmetries

There are three fundamental symmetries that determine the symmetry class the Hamiltonian belongs to. They are time-reversal symmetry (TRS), particle-hole symmetry (PHS) and chiral symmetry (CS). They are defined as:

$$\text{TRS: } TH^{\mathrm{T}}(-\mathbf{k},-t)T^\dagger = H(\mathbf{k},t)\,, \tag{4}$$

$$\text{PHS: } CH^{*}(\mathbf{k},t)C^\dagger = -H(-\mathbf{k},t)\,, \tag{5}$$

$$\text{CS: } \Gamma H^{*}(\mathbf{k},t)\Gamma^\dagger = -H(-\mathbf{k},t)\,. \tag{6}$$

If the Hamiltonian is static, in the definitions we can simply omit the time-dependence. For Hermitian Hamiltonians, TRS as per (4) is equivalent to the more frequent definition with complex conjugation instead of the transpose of the Hamiltonian. For non-hermitian Hamiltonians this is not true anymore. There is TRS and TRS†. TRS as defined in (4) is in fact TRS† according to K. Kawabata *et al.* ([14]). The same goes for PHS/CS, which as defined in (5)/(6), is in fact PHS†/CS†. However, we will abuse of notation and refer to the symmetries without dagger, simply by TRS, PHS and CS.

It is easy to see that the model defined in Eq. (1) has only TRS with $T = \mathbb{1}$, so it belongs to the AI symmetry class, according to the Altland-Zirnbauer classification [15]. If the driving amplitude is zero, we obtain the static SSH model, which belongs to the BDI class.

The zx model has TRS with $T = \sigma_z$ and PHS with $C = \sigma_x$. As CS is the product of TRS with PHS, then it also has CS, with $\Gamma = \sigma_y$. Hence, the zx model belongs to the BDI symmetry class.

As the xy model is a cyclic permutation of the Pauli matrices, it belongs to the BDI symmetry class as well, but with $T = \mathbb{1}$, $C = \sigma_z$ and $\Gamma = \sigma_z$.

B. Phase Diagram of the driven SSH model

The model defined in Eq. (1), as we stated, belongs to the AI symmetry class, which according to the periodic

table of Floquet topological insulators and superconductors in [15] has no topological invariant in one dimension. What we can do is compute the effective Magnus Hamiltonian [16] up to first order, valid for high frequencies, which yields ($\hbar = 1$)

$$H_{\text{eff}}(k) = H_0(k) + \frac{1}{\Omega}[H_1(k), H_1^\dagger(k)] = H_0(k) - \frac{4A^2}{\Omega}\sigma_1 = \\ = (t_1^{\text{eff}} + t_2 \cos k)\ \sigma_x + t_2 \sin k\ \sigma_y\,, \tag{7}$$

where $H_1(k)$ is the first (and only) harmonic component of the Hamiltonian (1), and $t_1^{\text{eff}} = t_1 - 4A^2/\Omega$. The effective Magnus Hamiltonian is just a static SSH Hamiltonian, with hopping terms t_1^{eff} and t_2. The phase diagrams for this Hamiltonian are presented in Fig. 1, where the topological invariant, the winding number ν [17], is plotted against the amplitude and period of the driving.

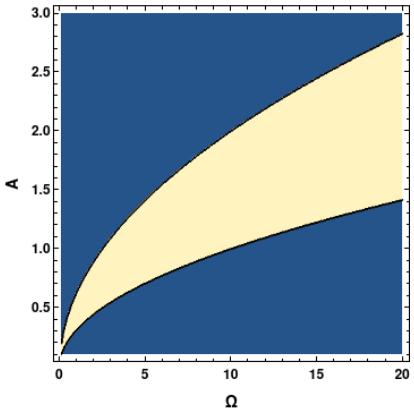

(a) $t_1 = 1$, $t_2 = 0.6$

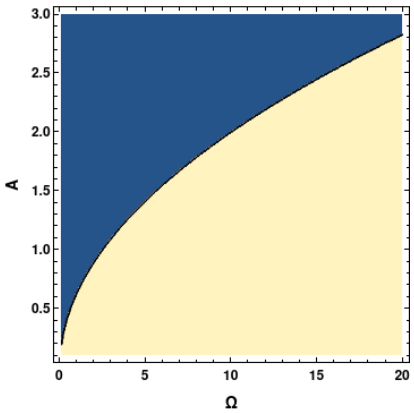

(b) $t_1 = 0.6$, $t_2 = 1$

FIG. 1: Phase diagram of the effective first order Magnus Hamiltonian of the driven SSH model. Blue: $\nu = 0$; White: $\nu = 1$.

One must take care when reading the phase diagrams of Fig. 1, since the Magnus expansion only makes sense for high frequencies. For mid-range and low frequencies the phase diagrams have no meaning. Furthermore, we are using a winding number best suited for static systems. So the winding number of the effective Hamiltonian does not capture the full picture. Additionally, this winding does not predict the existence of π-modes. As this model has no (dynamic) winding number, next we move on to the zx model, which has dynamical winding number.

C. Phase Diagram of the zx model

The zx model defined in Eq. (2), as we stated, belongs to the BDI symmetry class, which in one dimension has a winding number at the zero gap, ν_0, and a winding number at the π gap, ν_π, according to the periodic table of Floquet topological insulators and superconductors in Ref. [15].

In Fig. 2 the phase diagram of the zx model for $\mu = 0.5$ is shown. Each topological phase is characterized by the pair (ν_0, ν_π).

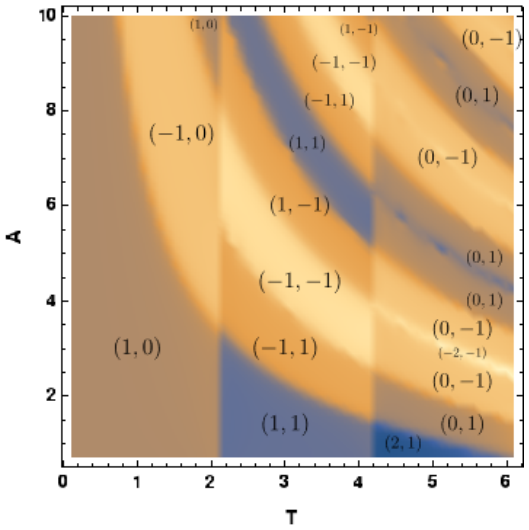

FIG. 2: Phase diagram of the zx model, for $\mu = 0$. A and T are the amplitude and period of the driving, respectively.

IV. CHARGE AND HEAT CURRENT

In this section we discuss briefly how to compute the average directed charge current and the average directed heat current. We start with the charge current. The electronic states in the chain obey the Floquet equation

$$i\hbar\partial_t|u_\epsilon(t)\rangle = [H(t) + \Sigma - \epsilon]|u_\epsilon(t)\rangle\,, \tag{8}$$

where $H(t)$ is the Hamiltonian of the chain in real space, ϵ is the quasi-energy and

$$\Sigma = -\frac{i}{2}[\Gamma_L|1\rangle\langle 1| + \Gamma_R|N\rangle\langle N|] \tag{9}$$

is the self-energy, which comes from the coupling of the chain to the leads. We work in the wide-band limit where Γ_L and Γ_R are constants.

The Fourier series of the Floquet state reads

$$|u_\epsilon(t)\rangle = \sum_{n\in\mathbb{Z}} e^{-in\Omega t}|u_n(\epsilon)\rangle\,. \tag{10}$$

Expanding the Hamiltonian of the chain as $H(t) = \sum_n H_n e^{in\Omega t}$, the Fourier components $|u_n(\epsilon)\rangle$ of the Floquet state obey

$$\sum_{n\in\mathbb{Z}}[H_{n-m} - n\hbar\Omega\delta_{n,m}]|u_n(\epsilon)\rangle = \epsilon|u_n(\epsilon)\rangle\,. \tag{11}$$

Because the Hamiltonian we work with includes a non-hermitian term, the quasienergies are complex. The Floquet states with quasienergies ϵ and $\epsilon+\hbar\Omega$ are physically the same, so we assume that $-\hbar\Omega/2 < \Re(\epsilon) \leq \hbar\Omega/2$. We call this interval the Floquet zone (FZ). Furthermore, we need to compute the left eigenstates, $|u^+_\epsilon(t)\rangle$, which obey

$$-i\hbar\partial_t\langle u^+_\epsilon(t)| = \langle u^+_\epsilon(t)|[H(t)+\Sigma-\epsilon]\,, \tag{12}$$

which in terms of Fourier components reads

$$\sum_{n\in\mathbb{Z}}\langle u^+_n(\epsilon)|[H_{n-m} - n\hbar\Omega\delta_{n,m}] = \langle u^+_n(\epsilon)|\epsilon\,. \tag{13}$$

The normalization condition $\sum_n\langle u^+_n(\epsilon)|u_n(\epsilon)\rangle = 1$ is satisfied. The orthonormality and completeness of the left and right eigenvectors basis vectors implies for the lattice sites $|j\rangle$ that

$$\sum_\epsilon\sum_{n\in\mathbb{Z}}\langle i|u_n(\epsilon)\rangle\langle u^+_n(\epsilon)|j\rangle = \langle i|j\rangle = \delta_{i,j}\,. \tag{14}$$

The electrical current flowing through the chain averaged in one cycle, in the wide-band limit, is given by [10]

$$\bar{I} = \frac{e}{h}\Gamma_L\Gamma_R\sum_{n\in\mathbb{Z}}\int \mathrm{d}E\,[|\mathcal{G}^{(n)}_{1N}(E)|^2 f_R(E) - |\mathcal{G}^{(n)}_{N1}(E)|^2 f_L(E)]\,, \tag{15}$$

where $-e$ is the electron charge, h the Planck's constant, and the functions $f_R(E)$ and $f_L(E)$ are the distribution functions of the leads. We assume both leads are in thermal equilibrium, so the electronic distribution function is the Fermi-Dirac function, the right one with chemical potential μ_R and the left one with chemical potential μ_L. $\mathcal{G}^{(n)}_{ij}(E)$ denotes the Green function

$$\mathcal{G}^{(n)}_{ij}(E) = \sum_{\epsilon\in\mathrm{FZ}}\sum_{m\in\mathbb{Z}}\frac{\langle i|u_{n+m}(\epsilon)\rangle\langle u^+_m(\epsilon)|j\rangle}{E-\epsilon-\hbar m\Omega}\,, \tag{16}$$

where the sum in the quasienergies is over the quasienergies in the Floquet zone. We work in the wide-band limit at zero temperature, so the distribution functions are stepwise, hence the integrands in (15) are rational functions and the integral can be done analytically. Besides the average current, experimentally we can also measure the differential conductance. In the zero temperature approximation the differential conductance fixing μ_L and raising μ_R, denoted by G_{LR}, is given by

$$\begin{aligned} G_{LR}(E) = \frac{\delta\bar{I}}{\delta V} &= \frac{\bar{I}(E+dE,E)-\bar{I}(E,E)}{\delta V} = \\ &= \frac{e^2}{h}\sum_{n\in\mathbb{Z}}T^{(n)}_{LR}(E) = \frac{e^2}{h}\Gamma_L\Gamma_R\sum_{n\in\mathbb{Z}}|\mathcal{G}^{(n)}_{1N}(E)|^2 \equiv \\ &\equiv \frac{e^2}{h}T_{LR}(E)\,. \end{aligned} \tag{17}$$

We could also define a differential conductance, G_{RL}, where we fix μ_R and lower μ_L. We would obtain

$$\begin{aligned} G_{RL}(E) &= \frac{e^2}{h}\sum_{n\in\mathbb{Z}}T^{(n)}_{RL}(E) = \frac{e^2}{h}\Gamma_L\Gamma_R\sum_{n\in\mathbb{Z}}|\mathcal{G}^{(n)}_{N1}(E)|^2 \equiv \\ &\equiv \frac{e^2}{h}T_{RL}(E)\,. \end{aligned} \tag{18}$$

If we want to study the charge pumping, we compute (15) with the leads at the same chemical potential. With $\mu_R = \mu_L = \mu_l$, the leads share the same distribution function $f(E)$, since we consider that they are at the same temperature. Hence, the pumped charge over a cycle, Q, is given by the average current at zero bias multiplied by the driving period, that is,

$$Q = \frac{e}{\hbar\Omega}\Gamma_L\Gamma_R\sum_{n\in\mathbb{Z}}\int \mathrm{d}E\; f(E)[|\mathcal{G}^{(n)}_{1N}(E)|^2 - |\mathcal{G}^{(n)}_{N1}(E)|^2]\,. \tag{19}$$

As we will need later on to study the even/odd behavior of the charge pumping, we compute the derivative of the pumped charge with respect to the chemical potential μ_l at zero temperature, which reads

$$Q'(\mu_l) = \frac{e}{\hbar\Omega}\Gamma_L\Gamma_R\sum_{n\in\mathbb{Z}}[|\mathcal{G}^{(n)}_{1N}(\mu_l)|^2 - |\mathcal{G}^{(n)}_{N1}(\mu_l)|^2]\,. \tag{20}$$

The heat $\mathcal{Q}_\alpha$ entering the lead α ($= L$ or R) per unit time with all leads at the same chemical potential μ_l is given by [13]

$$\begin{aligned} \dot{\mathcal{Q}}_\alpha = \frac{1}{h}\int \mathrm{d}E\sum_\beta\sum_{n\in\mathbb{Z}}(E-\mu_l+n\hbar\Omega)\Big\{&|S_{\alpha\beta}(n,E)|^2 f_\beta(E) - \\ &(E-\mu_l)|S_{\beta\alpha}(n,E)|^2 f_\alpha(E)\Big\}\,, \end{aligned} \tag{21}$$

where S is the Floquet scattering matrix. $S_{\alpha\beta}(n,E)$ is the probability amplitude for an incident wave with energy E leaving lead β to absorb ($n>0$) or emit ($n<0$) $|n|$ photons and leave through lead α with energy $E+n\hbar\Omega$. The Floquet scattering matrix is related to the Green function through

$$|S_{\alpha\beta}(n,E)|^2=\Gamma_\alpha\Gamma_\beta|\mathcal{G}^{(n)}_{\alpha\beta}(E)|^2\,. \tag{22}$$

Now we can either look at the total heating in one cycle $(\dot{\mathcal{Q}}_R+\dot{\mathcal{Q}}_L)2\pi/\Omega\equiv\mathcal{Q}_R+\mathcal{Q}_L$ or at the pumped heat between the leads in one cycle $(\dot{\mathcal{Q}}_R-\dot{\mathcal{Q}}_L)2\pi/\Omega\equiv\mathcal{Q}_R-\mathcal{Q}_L$. From Eq. (21) we have for the total heat and pumped heat

$$\mathcal{Q}_R+\mathcal{Q}_L=\mathcal{Q}_{1,+} \tag{23}$$
$$\mathcal{Q}_R-\mathcal{Q}_L=\mathcal{Q}_{1,-}+\mathcal{Q}_2\,, \tag{24}$$

where we defined for convenience

$$\mathcal{Q}_{1,\pm}=\sum_{n\in\mathbb{Z}}\int \mathrm{d}E\; f(E)n\left[|S_{RR}(n,E)|^2\;\pm|S_{LL}(n,E)|^2\right.$$
$$\left.+\;|S_{RL}(n,E)|^2\pm|S_{LR}(n,E)|^2\right]\,, \tag{25}$$
$$\mathcal{Q}_2=2\sum_{n\in\mathbb{Z}}\int \mathrm{d}E\; f(E)\left(\frac{E-\mu_l}{\hbar\Omega}\right)\left[|S_{RL}(n,E)|^2\right.$$
$$\left.-|S_{LR}(n,E)|^2\right]\,. \tag{26}$$

The terms in LL and RR are reflection terms not present in the charge current, which describe a heating effect caused by the radiation field on each lead when the fermions enter the chain through one lead, exchange photons with the radiation field, and return to same lead.

The term that has the energy in the numerator in (26) diverges logarithmically with the band-width of the electrode. Nonetheless, at zero temperature, the integral is from $-\infty$ to μ_l. The integral from $-\infty$ to 0 does not depend on μ_l, so we can discard it, and only the integral from 0 to μ_l remains. We compute the derivative of $\mathcal{Q}_{1,\pm}$ and $\mathcal{Q}_2$ with respect to the chemical potential separately, that read

$$\mathcal{Q}'_{1,\pm}(\mu_l)=\sum_{n\in\mathbb{Z}}n[|S_{RR}(n,\mu_l)|^2\pm|S_{LL}(n,\mu_l)|^2$$
$$+\;|S_{RL}(n,\mu_l)|^2\pm|S_{LR}(n,\mu_l)|^2] \tag{27}$$

and

$$\mathcal{Q}'_2(\mu_l)=-2\sum_{n\in\mathbb{Z}}\int_0^{\mu_l}\frac{\mathrm{d}E}{\hbar\Omega}\left[|S_{RL}(n,E)|^2-|S_{LR}(n,E)|^2\right] \tag{28}$$

The expressions above will determine if the behavior of both total heat and pumped heat as functions of the chemical potential are even or odd.

V. TOPOLOGY AND TRANSPORT

In this section we present our results of the study on the topological signatures in the transport properties of one-dimensional Floquet systems. We first consider the model defined in Eq. (1), and then the zx model.

A. Driven SSH model

In Fig. 3 the average current is plotted against the driving amplitude while fixing all the other parameters.

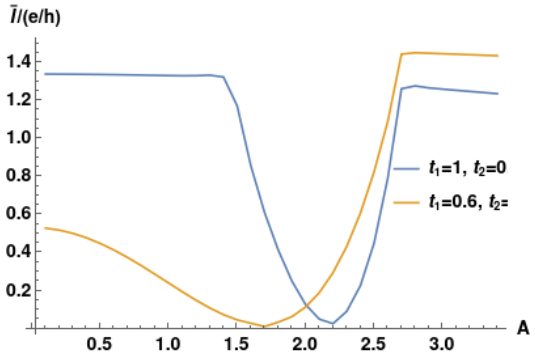

FIG. 3: Average current through the wire as a function of A. $\Omega=20$, $\Gamma_L=\Gamma_R=0.5$, $\mu_R=-\mu_L=25$. 80 sites.

We can see in these plots transitions between topological phases. In Fig. 1a the average current behaves monotonically for $A\lesssim 1.4$ and for $A\gtrsim 2.7$, while for $1.4\lesssim A\lesssim 2.7$ it decreases and then increases. In Fig. 1b we see only one transition around $A\approx 2.7$. For $A\lesssim 2.7$ the average current first decreases and then increases until it reaches the transition point. From that point on it behaves monotonically. Looking at Fig. 1 we see that these transitions occur when the value of the winding number changes.

B. zx model

As explained in [11], when the length of the topological insulator is finite, the topological states hybridize with bulk states and create additional transport channels across the structure. Thus a fingerprint of those states we expect to see is the existence of transmission peaks at the chemical potentials 0 whenever $\nu_0\neq 0$ or at $\pm\pi/T$ whenever $\nu_\pi\neq 0$ for homogeneous chains.

We choose Hamiltonian parameters so that the chain is in a homogeneous topological phase with edge states localized at sites $|1\rangle$ and $|N\rangle$. We also study the inhomogeneous system where the two halves of the chain are illuminated with two different amplitudes and are in two different topological phases. In this situation, localized states emerge in the middle of the chain, according to the bulk-edge correspondence principle.

So we do an analysis similar to the one done by H. Johansson and O. Balabanov in Ref. [11], which consists in studying the growth of the transmission peaks with the chain size. Here we consider homogeneous and inhomogeneous chains.

First we consider a situation where the left side of the chain is in the phase $(1,0)$ and the the right one is in the phase $(-1,0)$, such that we have four zero-energy bound states in total, according to the bulk-edge correspondence. We can see in Fig. 4 that the transmission peak at zero energy of the inhomogeneous chain survives for bigger chain sizes than the ones of the homogeneous chains.

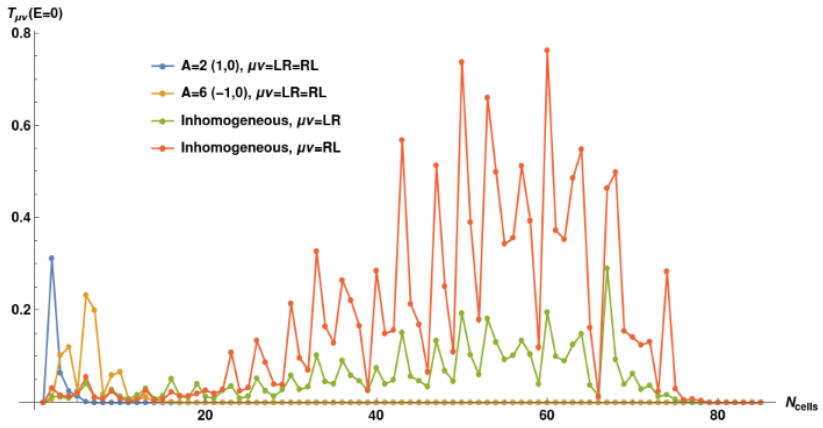

FIG. 4: Transmission peaks at zero chemical potential as a function of the number of unit cells, for homogeneous and inhomogeneous chains. Note that for the homogeneous chains $T_{LR}(0) = T_{RL}(0)$. $\mu = 0.5$, $T = 1.6$, $\Gamma_L = \Gamma_R = 0.5$, $A_L = 2$, $A_R = 6$.

To see what happens to the transmission peaks at the $\pm\pi$ energies we give an example with the left portion of the chain in the phase $(0,1)$ and the left one in the phase $(0,-1)$, so that we have four π-modes, according to the bulk-edge correspondence. Now we have to look for peaks at the chemical potentials $-\pi$ and π. We see from Fig. 5 that the peaks at $\pm\pi$ of the inhomogeneous chain survive for bigger chain sizes compared to the homogeneous cases, except for $T_{LR}(-\pi/T)$ of Fig. 5c. Nonetheless, we note that for inhomogeneous chains the peaks at zero chemical potential survive for bigger chain sizes compared to the peaks at $\pm\pi$.

The conclusion to make is that additional bound states enhance the conductivity, since there are more states which through tunnel effect occurs.

VI. SYMMETRIES AND CHARGE PUMPING

In this section we study the role symmetries play on the properties of charge pumping.

In this section and the next one parity symmetry (PS) will play a significant role, so we define it now as:

$$H(k,t) = PH(-k,t)P^\dagger\,, \text{ in momentum space,} \quad (29)$$
$$H(-x,t) = PH(x,t)P^\dagger\,, \text{ in real space.} \quad (30)$$

First we consider the zx model defined in (2). Although the Hamiltonian of the chain enjoys PS with $P = \sigma_z$, the coupling to the leads, Σ, violates PS, so one expects to have charge pumping. The leads break PHS symmetry as well. If the chain is inhomogeneous, then it is certain that PS is broken, so we will have charge pumping as well. If the chain is homogeneous, the pumped charge as a function of the chemical potential is even, as can be seen in the left panel of Fig. 6. This happens because the homogeneous chain enjoys the product of PS and PHS, we call it $\mathcal{PC}$ symmetry. For instance, starting from the Floquet equation and then applying the particle hole transformation followed by the parity transformation we obtain

$$i\hbar\partial_t|u_\epsilon(t)\rangle = [H_{zx}(t) + \Sigma - \epsilon]|u_\epsilon(t)\rangle \Leftrightarrow$$
$$\Leftrightarrow i\hbar\partial_t PC|u_\epsilon(-x,t)\rangle^* = [H_{zx}(x,t) + \Sigma + \epsilon^*]PC|u_\epsilon(-x,t)\rangle^*\,, \quad (31)$$

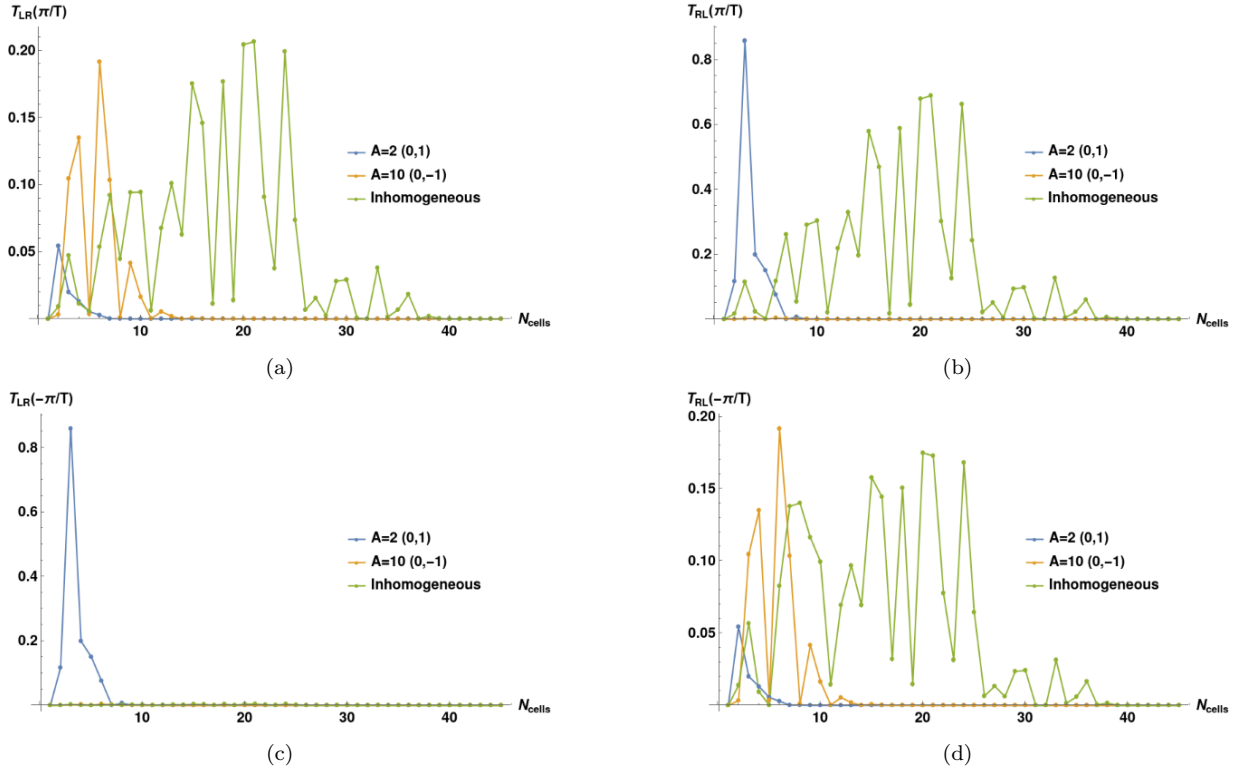

FIG. 5: Transmission peaks at chemical potentials $\pm\pi$ as a function of the number of unit cells, for homogeneous and inhomogeneous chains. (a) Left-right transmission coefficient at π. (b) Right-left transmission coefficient at π. (c) Left-right transmission coefficient at $-\pi$. (d) Right-left transmission coefficient at $-\pi$. $\mu = 1.5$, $T = 1.6$, $\Gamma_L = \Gamma_R = 0.5$, $A_L = 2$, $A_R = 10$.

where we used the fact that $PC\Sigma^*(-x)C^\dagger P^\dagger = -\Sigma(x)$ with $\Gamma_L = \Gamma_R$. Hence, the Floquet state $PC|u_\epsilon(-x,t)\rangle^*$ has quasienergy $-\epsilon^*$. So we have

$$PC|u_\epsilon(-x,t)\rangle^* = |u_{-\epsilon^*}(x,t)\rangle\,, \tag{32}$$

resulting for the Fourier components in

$$PC|u_{-n}(-x,\epsilon)\rangle^* = |u_n(x,-\epsilon^*)\rangle\,. \tag{33}$$

Since $PC = i\sigma_y$, we have in particular

$$\langle N|u_{-n}(\epsilon)\rangle^* = \langle N-1|PC|u_{-n}(\epsilon)\rangle^* = \langle 1|u_n(-\epsilon^*)\rangle^*, \tag{34}$$

$$\langle 1|u_{-n}(\epsilon)\rangle^* = -\langle 2|PC|u_{-n}(\epsilon)\rangle^* = -\langle N|u_n(-\epsilon^*)\rangle\,. \tag{35}$$

For the Green function this results in

$$\begin{aligned}\mathcal{G}^{(m)}_{1N}(E) &= \sum_{\epsilon\in \mathrm{FZ}}\sum_{n\in\mathbb{Z}} \frac{\langle 1|u_{m+n}(-\epsilon^*)\rangle\langle u^+_n(-\epsilon^*)|N\rangle}{E+\epsilon^*-\hbar n\Omega} = \\ &= -\sum_{\epsilon\in \mathrm{FZ}}\sum_{n\in\mathbb{Z}} \frac{\langle N|u_{-m-n}(\epsilon)\rangle^*\langle u^+_{-n}(\epsilon)|1\rangle^*}{E+\epsilon^*-\hbar n\Omega} = \\ &= \left(\mathcal{G}^{(-m)}_{N1}(-E)\right)^*\,. \end{aligned} \tag{36}$$

If we use the previous relation in Eq. (20), we arrive at $Q'(\mu_l) = -Q'(-\mu_l)$, which implies that the pumped charge is an even function of the chemical potential.

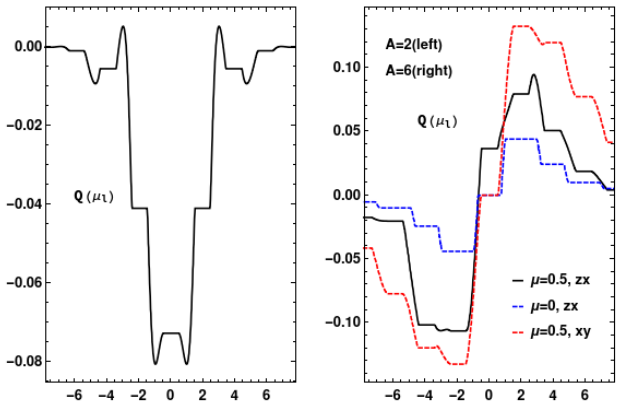

FIG. 6: Charge pumped in a cycle vs. chemical potential, in a homogeneous xz model chain (left panel), and in inhomogeneous chains of the zx and xy models (right panel), where two halves of the chain are illuminated with different amplitudes. The parameters are $T = 1.6$, $\Gamma_L = \Gamma_R = 0.5$, 60 sites. $A = 2$ and $\mu = 0.5$ for the left panel.

In the right panel of Fig. 6 the pumped charge is

plotted against the chemical potential for inhomogeneous chains of the zx and xy model. Considering first the zx model, we note that for $\mu = 0$, when two halves of the chain are driven with different amplitudes, the pumped charge is an odd function of the chemical potential. The $\mathcal{PC}$ symmetry is explicitly broken, but the system has a special kind of PHS that only strictly holds when $\mu = 0$. We introduce the operator $\mathcal{O}$ which acts upon the Floquet state in space-time domain as $\mathcal{O}|u(x,t)\rangle = (-1)^x|u(x,t+\pi/\Omega)\rangle$. In momentum-time space, $\mathcal{O}$ produces a wave vector shift $k \to k+\pi$ and time translation by half a period. If we now consider the operator $\sigma_3\mathcal{O}\mathcal{K}$, where $\mathcal{K}$ denotes the complex conjugation, we see that

$$\sigma_z\mathcal{O}\left[H^*_{zx}(-k,t)\right]_\mu\mathcal{O}^{-1}\sigma_z = -\left[H^*_{zx}(k,t)\right]_{-\mu}\,, \tag{37}$$

while for the self-energy

$$\sigma_z\mathcal{O}\Sigma^*\mathcal{O}^{-1}\sigma_z = -\Sigma\,. \tag{38}$$

Eqs. (37) and (38) show that $\sigma_3\mathcal{O}$ serves as modified form of PHS when $\mu = 0$. The effect of $\sigma_3\mathcal{O}\mathcal{K}$ on the Floquet equation is (here we drop the label zx in the chain's Hamiltonian)

$$\begin{gathered} i\hbar\partial|u_\epsilon(t)\rangle = \left[H(t)+\Sigma-\epsilon\right]|u_\epsilon(t)\rangle \\ \Leftrightarrow i\hbar\sigma_z\mathcal{O}\partial|u_\epsilon(t)\rangle^* = \left[H_{-\mu}(t)+\Sigma+\epsilon^*\right]\sigma_z\mathcal{O}|u_\epsilon(t)\rangle^*\,. \end{gathered} \tag{39}$$

Therefore, the state $\sigma_z\mathcal{O}|u_\epsilon(t)\rangle^*$ has quasi-energy $-\epsilon^*$ in the Hamiltonian $H_{-\mu}(t)+\Sigma$. In terms of the Fourier components of the Floquet function

$$\begin{aligned} \sigma_z\mathcal{O}|u_\epsilon(x,t)\rangle^*(x,t) &= \sum_n \sigma_z|u_n(x,\epsilon)\rangle^*(-1)^{x+n}e^{in\Omega t} = \\ &= \sum_n \sigma_z|u_{-n}(x,\epsilon)\rangle^*(-1)^{x+n}e^{-in\Omega t} = |u_{-\epsilon^*}(x,t)\rangle\,. \end{aligned} \tag{40}$$

We are now able to compute the Green function's matrix elements when μ is replaced by $-\mu$:

$$\begin{aligned} \left[\mathcal{G}^{(m)}_{1N}(E)\right]_{-\mu} &= \sum_{\epsilon\in\mathrm{FZ}}\sum_{n\in\mathbb{Z}}\frac{\langle 1|u_{m+n}(-\epsilon^*)\rangle\langle u^+_n(-\epsilon^*)|N\rangle}{E+\epsilon^*-n\hbar\Omega} \\ &= \sum_{\epsilon\in\mathrm{FZ}}\sum_{n\in\mathbb{Z}}\frac{\langle 1|\sigma_z\mathcal{O}u_{-m-n}(\epsilon)\rangle^*\langle\sigma_z\mathcal{O}u^+_{-n}(\epsilon)|N\rangle^*}{E+\epsilon^*-n\hbar\Omega} \\ &= \sum_{\epsilon\in\mathrm{FZ}}\sum_{n\in\mathbb{Z}}\frac{(-1)^{m+\frac{N}{2}}\langle 1|u_{-m+n}(\epsilon)\rangle^*\langle u^+_n(\epsilon)|N\rangle^*}{E+\epsilon^*+n\hbar\Omega} \\ &= (-1)^{1+m+N/2}\left[\mathcal{G}^{(-m)}_{1N}(-E)\right]^*_\mu\,. \end{aligned} \tag{41}$$

When $\mu = 0$ we have $|\mathcal{G}^{(m)}_{1N}(E)|^2 = |\mathcal{G}^{(-m)}_{1N}(-E)|^2$. From (20) we can see that $\mathcal{Q}'(\mu_l)$ is an even function, which implies that the pumped charge is odd. This explains the result from the right panel of Fig. 6. If $\mu \neq 0$ neither $\mathcal{PC}$ nor PHS' are present, so the pumped charge is neither even nor odd. In the homogeneous case, if $\Gamma_L \neq \Gamma_R$ the $\mathcal{PC}$ symmetry is broken, so when $\mu \neq 0$ the pumped charge is no longer an even function of the chemical potential. Nonetheless, if $\mu = 0$ the pumped charge is an odd function, because PHS' is present.

Now we turn to the xy model, where $P = \sigma_x$ and $C = \sigma_z$. In the homogeneous case, the leads preserve PS if $\Gamma_L = \Gamma_R$, so there is no charge pumping. However, in the inhomogeneous case we have charge pumping. The PS of the system is broken, but PHS is still preserved. Indeed, $CH^*_{xy}(t)C^\dagger = -H_{xy}(t)$ and $C\Sigma^*C^\dagger = -\Sigma$, and the Floquet equation for the Floquet state $|u_\epsilon(t)\rangle$ with quasienergy ϵ reads

$$\begin{gathered} i\hbar\partial_t|u_\epsilon(t)\rangle = \left[H_{xy}(t)+\Sigma-\epsilon\right]|u_\epsilon(t)\rangle \Leftrightarrow \\ \Leftrightarrow i\hbar\partial_t C|u_\epsilon(t)\rangle^* = \left[H_{xy}(t)-C\Sigma^*C^\dagger+\epsilon^*\right]C|u_\epsilon(t)\rangle^*\,, \end{gathered} \tag{42}$$

and since $C\Sigma^*C^\dagger = -\Sigma$, the state $C|u_\epsilon(t)\rangle^*$ has quasienergy $-\epsilon^*$ for the Hamiltonian $H_{xy}(t) - C\Sigma^*C^\dagger = H_{xy}(t)+\Sigma$, which means that

$$C|u_\epsilon(t)\rangle^* = |u_{-\epsilon^*}(t)\rangle\,. \tag{43}$$

For the Fourier components it reads

$$\sigma_z|u_{-n}(\epsilon)\rangle = |u_n(-\epsilon^*)\rangle \Leftrightarrow |u_n(\epsilon)\rangle = \sigma_z|u_{-n}(-\epsilon^*)\rangle\,. \tag{44}$$

Using the previous equation in (16) we get

$$\mathcal{G}^{(m)}_{1N}(E) = \sum_{\epsilon\in\mathrm{FZ}}\sum_{n\in\mathbb{Z}}\frac{\langle 1|u_{-m-n}(-\epsilon^*)\rangle^*\langle u^+_{-n}(-\epsilon^*)|N\rangle^*}{E-\epsilon-\hbar n\Omega}\,. \tag{45}$$

Replacing $n \to -n$ and $\epsilon \to -\epsilon^*$ one can see that $\mathcal{G}_{1N}(m,E) = \mathcal{G}^*_{1N}(-m,-E)$, and a similar relation can be derived for $\mathcal{G}_{N1}$. It follows that the relation

$$|\mathcal{G}^{(m)}_{1N}(E)|^2 = |\mathcal{G}^{(-m)}_{1N}(-E)|^2 \tag{46}$$

holds, which means $Q'(\mu_l)$ is an even function, so the pumped charge is odd, just as can be seen in the right panel of Fig. 6. For a homogeneous chain with $\Gamma_L = \Gamma_R$ PS symmetry is present, so there is no charge pumping. If $\Gamma_L \neq \Gamma_R$, then PS is broken, hence there is charge pumping. As PHS is still present, the pumped charge is an odd function of the chemical potential.

VII. SYMMETRIES AND HEAT PUMPING

Now we study the role symmetries have on the heat flow. We know how to compute the total heat and the pumped heat over a cycle through Eqs. (23) and (24). We work in the wide-band limit at zero temperature, so the integrals can be done analytically. First we study the case of the homogeneous zx chain, which has $\mathcal{PC}$ symmetry. Similarly to (34) we have

$$\langle 1|u_n(-\epsilon^*)\rangle = \langle N-1|PC|u_{-n}(\epsilon)\rangle^* = -\langle N|u_{-n}(\epsilon)\rangle^*, \tag{47}$$

$$\langle u_n^+(-\epsilon^*)|1\rangle = \langle PCu_{-n}^+(\epsilon)|N-1\rangle^* = -\langle u_{-n}^+(\epsilon)|N\rangle^* . \tag{48}$$

using the previous relations in the Green function yields

$$\begin{aligned}\mathcal{G}_{11}^{(m)}(E) &= \sum_{\epsilon\in \mathrm{FZ}}\sum_{n\in\mathbb{Z}} \frac{\langle 1|u_{m+n}(-\epsilon^*)\rangle\langle u_n^+(-\epsilon^*)|1\rangle}{E+\epsilon^*-\hbar n\Omega} = \\ &= -\sum_{\epsilon\in \mathrm{FZ}}\sum_{n\in\mathbb{Z}} \frac{\langle N|u_{-m+n}(\epsilon)\rangle^*\langle u_n^+(\epsilon)|N\rangle^*}{-E-\epsilon^*-\hbar n\Omega} = \\ &= -\mathcal{G}_{NN}^{(-m)}(-E)\,. \end{aligned} \tag{49}$$

Besides having $|S_{LR}(n,E)|^2 = |S_{RL}(-n,-E)|^2$, we now have also $|S_{LL}(n,E)|^2 = |S_{RR}(-n,-E)|^2$, assuming $\Gamma_L = \Gamma_R$. In this way, the derivative of the total heat as in (27) (choosing the plus sign) verifies $(\mathcal{Q}_R+\mathcal{Q}_L)'(\mu_l) = -(\mathcal{Q}_R+\mathcal{Q}_L)'(-\mu_l)$. Hence, the total heat is an even function of μ_l. Se left panel of Fig. 7. Through Eq. (27) with the minus sign and Eq. (28), one can see that $(\mathcal{Q}_R-\mathcal{Q}_L)'(\mu_l) = (\mathcal{Q}_R-\mathcal{Q}_L)'(-\mu_l)$, which implies that the pumped heat is an odd function of μ_l, apart from a constant. See the right panel of Fig. 7.

If $\Gamma_L \neq \Gamma_R$, in the homogeneous case with $\mu \neq 0$, as functions of the chemical potential, the total heat is no longer an even function and the pumped heat is no longer and odd function (up to a constant), because in this way $\mathcal{PC}$ is broken. Nonetheless, if $\mu = 0$ PHS' is present. A similar reasoning that led to (41) yields $(ii = 11, NN)$

$$\left[\mathcal{G}_{ii}^{(m)}(E)\right]_{-\mu} = (-1)^{m+1}\left[\mathcal{G}_{ii}^{(-m)}(-E)\right]_{\mu}^* . \tag{50}$$

Eqs. (41) and (50) imply that $|S_{\alpha\beta}(n,\mu_l)|^2 = |S_{\alpha\beta}(-n,-\mu_l)|^2$ holds when $\mu = 0$. In this way, both $(\mathcal{Q}_R+\mathcal{Q}_L)'(\mu_l)$ and $(\mathcal{Q}_R+\mathcal{Q}_L)'(\mu_l)$ determined by Eqs. (27) and (28) are odd functions, which means PHS' renders both total heat and pumped heat even functions. If $\mu = 0$ and $\Gamma_L = \Gamma_R$ there is neither charge nor heat pumping, but there is total heat and it is an even function. In the inhomogeneous case with $\mu = 0$, $(\mathcal{Q}_R \pm \mathcal{Q}_L)(\mu_l)$ are even functions because PHS' is present. If $\Gamma_L \neq \Gamma_R$, $(\mathcal{Q}_R \pm \mathcal{Q}_L)(\mu_l)$ remain even, as long as $\mu = 0$. If $\mu \neq 0$ in the inhomogeneous case $(\mathcal{Q}_R \pm \mathcal{Q}_L)(\mu_l)$ are no longer even functions. See Fig. 8.

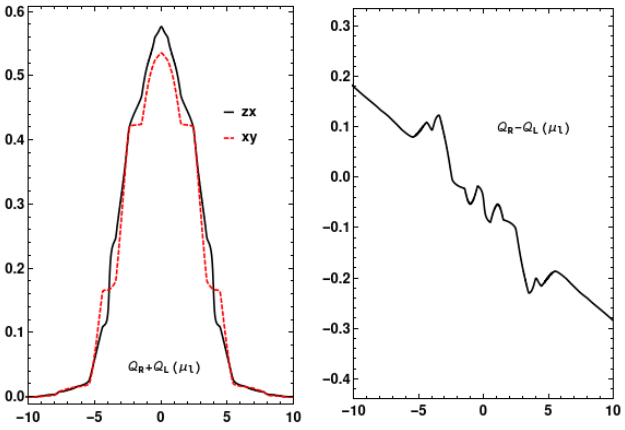

FIG. 7: Total heat (left panel) and pumped heat (right panel) in a cycle vs. chemical potential in homogeneous chains of the zx model (left and right panels) and of the xy model (left panel). The parameters are:$\mu = 0.5$, $A = 2$, $T = 1.6$, $\Gamma_L = \Gamma_R = 0.5$, 60 sites.

For a homogeneous chain of the xy model with $\Gamma_L = \Gamma_R$ PS symmetry is present, so there is no heat pumping. However, we have total heating, and it is an even function, as can be seen in the left panel of Fig. 7 (red dashed line). This happens because the chain has PHS, as it was already stated above. A similar reasoning that led to (45) leads to $(ii = 11, NN)$

$$\mathcal{G}_{ii}^{(m)}(E) = -\left(\mathcal{G}_{ii}^{(-m)}(-E)\right)^* , \tag{51}$$

which implies $|S_{\alpha\beta}(n,E)|^2 = |S_{\alpha\beta}(-n,-E)|^2$, so $(\mathcal{Q}_R \pm \mathcal{Q}_L)(\mu_l)$ are even functions, but in this case we have only total heating. If the chain is inhomogeneous, PS symmetry is broken, so we will have heat pumping. Nonetheless, PHS is still present, so $(\mathcal{Q}_R \pm \mathcal{Q}_L)(\mu_l)$ remain even functions, as can be seen in Fig. 8 (red lines).

VIII. CONCLUSIONS

In this work we studied the role of topology on the transport properties in one-dimensional Floquet systems and studied the role of symmetries on the charge and heat pumping as well.

First we considered a driven SSH chain in the AI symmetry class. We obtained the phase diagrams based on the winding number of the first order Magnus Hamiltonian. We saw that the average current behaves non-monotonically/monotonically when the system is the non-topological/topological phase. Then we computed the transmission peaks at zero energy for homogeneous and inhomogeneous chains of a model belonging to the BDI class we called zx model. In the inhomegeneous case two halves of the chain were illuminated with different driving amplitudes, being in different topological phases,

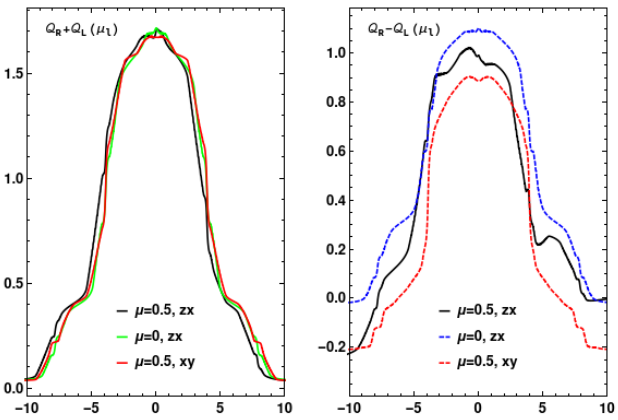

FIG. 8: Total heat (left panel) and pumped heat (right panel) in a cycle vs. chemical potential, in inhomogeneous chains of the zx and xy models. $A = 2$(left), $A = 6$(right), $T = 1.6$, $\Gamma_L = \Gamma_R = 0.5$, 60 sites.

with $|\nu_0^L - \nu_0^R| = 2$ and $\nu_\pi^L = \nu_\pi^R = 0$. The transmission peaks were computed varying the chain size, similarly to what was in [11].We found that the transmission peak at zero energy for inhomogeneous chains survives for bigger chain sizes compared to the case of homogeneous chains. This is due to the additional number of bound states, which opens additional channels for the electrons to tunnel across the chain. We repeated the procedure for a chain with $|\nu_\pi^L - \nu_\pi^R| = 2$ and $\nu_0^L = \nu_0^R = 0$, plotting the transmission peaks at $\pm\pi$ energies against the chain size. The transmission peaks of the inhomogeneous were observed to survive for bigger chain sizes compared to the homogeneous chains, except for $T_{LR}(-\pi/T)$. However, the peaks at $\pm\pi/T$ energies vanish for chain sizes smaller than the ones for which the peaks at zero vanish.

Then we focused on the study of charge and heat pumping. In the zx model the leads break PS, so we have charge pumping. The homogeneous chain with $\mu \neq 0$ does not have PHS, but has the product of PHS and PS, that renders the pumped charge an even function of the chemical potential and the pumped heat an odd function of the chemical potential. For $\mu = 0$ the system has also a special kind of particle-hole symmetry, which renders the pumped charge an odd function of the chemical potential and the pumped heat an even function. Thus, being even and odd functions of the chemical potential, the pumped charge and the pumped heat through homogeneous chains of the zx model with $\mu = 0$ are zero. Inhomogeneous chains of the zx model with $\mu \neq 0$ enjoy none of the symmetries considered. Thus the pumped charge and the pumped heat are neither even nor odd functions.When $\mu = 0$, the inhomogeneous chain enjoys PHS', so the pumped charge and the pumped heat are odd and even , respectively. In the other model called xy we considered, obtained by a permutation of the Pauli matrices of the xz model, the leads preserve PS, so there is neither pumped charge nor pumped heat for homogeneous chains. In inhomogeneous chains PS is broken, so we have charge and heat pumping. Only PHS symmetry is present, which in this case renders the pumped charge and the pumped heat odd and even, respectively. Basically, we can easily reverse the direction of the charge or heat flow by only tuning the chemical potential.

[1] T. Oka and H. Aoki, Phys. Rev. B **79**, 081406 (2009), URL https://link.aps.org/doi/10.1103/PhysRevB.79.081406.

[2] M. König *et al.*, Science **318**, 766 (2007).

[3] B. A. Bernevig, T. L. Hughes, and S.-C. Zhang, Science **314**, 1757 (2006), ISSN 0036-8075, URL https://science.sciencemag.org/content/314/5806/1757.

[4] R. Yu, W. Zhang, H. Zhang, and S. Zhang, Nature Physics **329**, 61 (2010).

[5] C. Chang *et al.*, Science **340**, 167 (2013).

[6] N. Lindner, G. Refael, and V. Galitski, Nature **7**, 490–495 (2011).

[7] T. Oka and H. Aoki, Phys. Rev. B **79**, 081406 (2009), URL https://link.aps.org/doi/10.1103/PhysRevB.79.081406.

[8] G. Jotzu, M. Messer, R. Desbuquois, M. Lebrat, T. Uehlinger, D. Greif, and T. Esslinger, Nature **515**, 237–240 (2014).

[9] F. Haldane, Phys. Rev. Lett. **61**, 2015 (1988), URL https://link.aps.org/doi/10.1103/PhysRevLett.61.2015.

[10] S. Kohler, J. Lehmann, and P. Hänggi, Physics Reports **406**, 379 (2005), ISSN 0370-1573, URL http://www.sciencedirect.com/science/article/pii/S0370157304005071.

[11] O. Balabanov and H. Johannesson, Journal of Physics: Condensed Matter **32**, 015503 (2019), URL https://doi.org/10.1088%2F1361-648x%2Fab4319.

[12] L. E. F. Foa Torres, Phys. Rev. B **72**, 245339 (2005), URL https://link.aps.org/doi/10.1103/PhysRevB.72.245339.

[13] M. Moskalets and M. Büttiker, Phys. Rev. B **66** (2002), URL https://link.aps.org/doi.org/10.1103/PhysRevB.66.205320.

[14] K. Kawabata, K. Shiozaki, M. Ueda, and M. Sato, Phys. Rev. X **9**, 041015 (2019), URL https://link.aps.org/doi/10.1103/PhysRevX.9.041015.

[15] S. Yao, Z. Yan, and Z. Wang, Phys. Rev. B **96**, 195303 (2017), URL https://link.aps.org/doi/10.1103/PhysRevB.96.195303.

[16] S. Rahav, I. Gilary, and S. Fishman, Phys. Rev. A **68**, 013820 (2003), URL https://link.aps.org/doi/10.1103/PhysRevA.68.013820.

[17] H.-T. Chen, C.-H. Chang, and H. chung Kao, *The zak phase and winding number* (2019), 1908.06700.